



Adsorption of aqueous cadmium (II) onto modified multi-walled carbon nanotubes following microwave/chemical treatment

Chao-Yin Kuo^{a,*}, Han-Yu Lin^b

^a Department of Safety Health and Environmental Engineering, National Yunlin University of Science and Technology, 123 University Rd., Sec. 3, Douliou, Yunlin 640, Taiwan

^b Graduate School of Engineering Science and Technology, National Yunlin University of Science and Technology, Taiwan

ARTICLE INFO

Article history:

Accepted 11 November 2008

Available online 4 October 2009

Keywords:

Microwave
Cadmium ion (II)
Carbon nanotubes
Adsorption

ABSTRACT

This study evaluates the aqueous cadmium (II) adsorption efficiency of as-grown carbon nanotubes (CNTs) and of those modified by microwave (MW)/H₂SO₄ and MW/H₂SO₄/KMnO₄ processes. The surface area, pH_{iep}, and FTIR spectra of CNTs were, before and after modification, compared. Aromatic groups, carbonyl groups and hydroxyl groups were herein detected on the surfaces of MW/H₂SO₄ and MW/H₂SO₄/KMnO₄-modified CNTs. At a particular pH, the adsorption capacity of Cd²⁺ of the MW/H₂SO₄/KMnO₄-modified CNTs exceeded that of MW/H₂SO₄-modified CNTs and as-grown CNTs. The kinetic analyses of adsorption were performed and a pseudo second-order model accurately captured the adsorption kinetics. This study suggests that MW/H₂SO₄ and MW/H₂SO₄/KMnO₄ modification not only increased the area of active adsorption sites of CNTs but also reduced the modification period by microwave heating.

© 2009 Elsevier B.V. All rights reserved.

1. Introduction

Removing toxic heavy metals from industrial wastewater is an urgent environmental issue. Heavy metals are non-degradable and can accumulate in animals and plants, so they must be removed from wastewater. Heavy metal ions such as cadmium (II) ions are the main contaminants of surface water, groundwater and soils; the main sources are the metal plating industry [1,2]. Due to their non-biodegradability and persistence, they can accumulate in the environment elements such as food chain, and thus may pose a significant danger to human health [2–5]. Exposure to cadmium (II) can result in osteoporosis, anaemia and renal damage [6,7]. However, the use of cadmium in paint pigments, electroplating, batteries, is increasing.

Carbon nanotubes (CNTs) are new adsorbents of trace pollutants from water, because they have a large specific surface area, and small, hollow and layered structures. Considerable attention has been paid to adsorption by CNTs of such ions as Cd²⁺. Earlier works have suggested that CNTs may be a potential adsorbent for treating wastewater [8–15]. Hence, numerous approaches to the purification or enhancement of functional groups on CNTs that involve separation and elimination processes have been developed [12–15]. They fall into two groups according to the general mechanism of functionalization of CNTs. In the first, some C=C bonds are fully opened, forming defects within the CNT wall; in the second, some C=C bonds are broken and single bonds are used for functionalization, yielding some sp³ character of particular C atoms. The oxidation of carbon surfaces is known to generate

not only more hydrophilic surface structures but also more oxygen-containing functional groups and to increase the ion-exchange capacity [13]. The first type of functionalization typically involves oxidation using acids or oxidants [13–15], causing carboxyl groups to functionalize the defects and the ends of the CNTs [12]. The second type CNT wall functionalization is generally an addition of a C=C double bond by alkylation, arylation, oxycarbonyl nitrene, and 1,3 dipolar cyclo-addition [16–19]. Such reactions are normally time-consuming, taking hours or even days. In organic chemistry, particular reactions can be microwave-assisted to increase selectivity and reduce reaction times [13,15,20], sometimes from days to a few minutes [13,15]. The present study reported a multi-walled CNT functionalization method that involves microwave assistance.

This study elucidates the equilibrium of the adsorption of Cd²⁺ onto CNTs. The Cd²⁺ adsorption capacity is increased by modifying the surfaces of MW/H₂SO₄ and MW/H₂SO₄/KMnO₄. The aims of this study are (i) to identify and compare the surfaces of as-grown, MW/H₂SO₄-modified and MW/H₂SO₄/KMnO₄-modified CNTs; (ii) to determine the effects of pH and temperature on the adsorption of Cd²⁺ by as-grown and modified CNTs; and (iii) to evaluate the adsorption rate using kinetic models.

2. Materials and methods

The as-grown CNTs herein were multi-wall CNTs (CBT, MWNTs-2040, length: 5–15 μm, purity of carbon: above 90%). They were formed by the pyrolysis of methane gas on particles of Ni by chemical vapor deposition. The Cd²⁺ stock solution was prepared from Cd(NO₃)₂·3H₂O and Milli-Q deionized water. The zeta potentials of the

* Corresponding author. Tel.: +886 5 534 5601x4423; fax: +886 5 531 2069.
E-mail address: kuocy@ms35.hinet.net (C.-Y. Kuo).

as-grown and oxidized CNTs were measured using a Zeta-Meter 3.0 (Zeta-Meter Inc., U.S.A.). The acidity or basicity of the CNTs surface and the isoelectric point of pH_{iep} were determined by measuring the zeta potential as a function of pH of the CNT solution from 2.0 to 9.0 at 300 K.

The functional groups of CNTs were identified by Fourier Transform Infrared Spectroscopy (FTIR) analysis and an autoimagic system (Perkin Elmer, USA) using the KBr pressed disc method. Scanning electron microscopic/energy dispersive X-ray spectroscopic (SEM/EDS) analyses (JEOL, JSM-T330A) yielded the number of oxygen and nickel atoms in as-grown and modified CNTs. The specific surface area of CNTs was measured using the BET method, using a Model ASAP 2010 surface area analyzer (Micromeritics, USA). The size and morphology of the CNTs were elucidated by transmission electron microscopy (TEM) using a Model JEM-2010 (JEOL, Japan).

The configuration of microwave is in a closed microwave oven system and the volumetric capacity of Teflon flasks of microwave oven is 100 ml. As-grown CNTs (1 g) were immersed in Teflon flasks with 20 ml of 1 M H_2SO_4 and 20 ml of 1 M H_2SO_4 adding 1 g of KMnO_4 then rotated in a microwave system (400 W) for 10 min in the modification of MW/ H_2SO_4 and MW/ $\text{H}_2\text{SO}_4/\text{KMnO}_4$. 10 min and the potency (400 W) were chosen in the modification of MW/ H_2SO_4 and MW/ $\text{H}_2\text{SO}_4/\text{KMnO}_4$ because of keeping the complete structure of CNTs against destruction. The modified CNTs were washed repeatedly in Milli-Q deionized water until the pH of the solution reached 7; finally, the modified CNTs were dried at 343 K for 12 h. All of the adsorption experiments were conducted in a closed 250 ml glass pyramid bottle, containing 0.05 g of as-grown or modified CNTs; 200 ml of Cd^{2+} solution (40 mg/l) was placed in a water bath. In experiments on the effect of pH, the pH of the solution was adjusted to between 2 and 9, using 0.1 M HNO_3 and 0.1 M NaOH and 0.01 M of solution ionic strength was controlled by NaNO_3 . In the experiments on the effect of adsorption in temperature, the temperature was maintained at 290, 300 and 310 K. Following sampling, the suspensions were centrifuged at 4000 rpm for 10 min, and the supernatant was then filtered through 0.2 μm filter paper for subsequent analysis of the Cd^{2+} concentration, using inductively coupled plasma-optical emission spectrometer (ICP-OES) with a Model OPTIMA 2100DV.

3. Results and discussion

3.1. Characteristics of CNTs

The pH_{iep} of as-grown CNTs and MW/ H_2SO_4 -modified CNTs was determined to be 4.9 and 3.8 (Table 1). The experimental results reveal that all of the zeta potentials of CNTs became more negative as the pH increased and the zeta potentials of the MW/ $\text{H}_2\text{SO}_4/\text{KMnO}_4$ -modified CNTs were all negative at pH 2–9. Various studies have demonstrated that the zeta potentials of modified CNTs are more negative than those of as-grown CNTs [10,14,21,22]. The specific surface areas of MW/ H_2SO_4 and MW/ $\text{H}_2\text{SO}_4/\text{KMnO}_4$ -modified CNTs exceeded that of as-grown CNTs, because of their exposed internal surface [10,21]. In Table 1, the calibrated SEM/EDS revealed 5.4, 7.8 and 12.2 at.% oxygen atoms and 1.0, 0.5 and 0.5 at.% nickel atoms in as-grown, MW/ H_2SO_4 -modified and MW/ $\text{H}_2\text{SO}_4/\text{KMnO}_4$ -modified CNTs, respectively. The results indicate that carboxyl and hydroxyl

formed on the surface of these-modified CNTs as the number of oxygen atoms increased.

The chemical modification of MWCNT with oxidant acids lead to increase of external diameters of the nano-materials [21]. The surface area was 78, 98 and 112 (m^2/g) in as-grown, MW/ H_2SO_4 -modified and MW/ $\text{H}_2\text{SO}_4/\text{KMnO}_4$ -modified CNTs, respectively and the external diameters were not increased due to the short microwave heating. The number of oxygen atoms on modified CNTs exceeded that on as-grown CNTs, revealing that the modification processes promoted the formation of the oxygenic functional groups on the modified surfaces of the CNTs. This observation was consistent with those of Li et al. [10], Kuo [15] and Monthieux et al. [23]. Accordingly, the experimental results indicate that oxidation treatments may have not only removed Ni particles and amorphous carbons but also produced some structural defects.

Fig. 1 displays the FTIR spectra of as-grown and modified CNTs. The as-grown CNTs yielded three peaks. A peak at near 1450–1600 cm^{-1} , which was assigned to the aromatic $-\text{C}-\text{C}$ groups [24], a peak at approximately 1700–1740 cm^{-1} , which was assigned to the carbonyl $-\text{C}=\text{O}$ groups [25] and a peak at about 3200–3400 cm^{-1} , which was assigned to the hydroxyl $-\text{OH}$ groups [24–26]. MW/ H_2SO_4 and MW/ $\text{H}_2\text{SO}_4/\text{KMnO}_4$ oxidation significantly increased this peak. Lu et al. [12] found that the chemical oxidation of CNTs introduces various acidic functional groups onto their surfaces, improving their hydrophilicity. The MW/ H_2SO_4 -modified CNTs yielded a peak at about 3200–3400 cm^{-1} , which was assigned to the aromatic $-\text{OH}$ groups. MW/ $\text{H}_2\text{SO}_4/\text{KMnO}_4$ -modified CNTs yielded four major peaks, which were associated with aromatic groups at 1450–1600 cm^{-1} , carbonyl groups at 1700–1740 cm^{-1} , carboxylic acids at 2400 cm^{-1} , $-\text{CH}$ groups at 2800–3100 cm^{-1} [24,26] and hydroxyl groups at 3200–3400 cm^{-1} —the latter two from carboxylic acids or alcoholic groups. Evidently, several functional groups were formed on the surface of modified CNTs, providing various adsorption sites, and increasing the adsorption capacity. Modification by MW/ $\text{H}_2\text{SO}_4/\text{KMnO}_4$ increased the discretization of CNTs, enlarging the external surface area of the CNTs. The TEM images revealed that the as-grown and modified CNTs were cylindrical and that the main external diameters of as-grown, MW/ H_2SO_4 and MW/ $\text{H}_2\text{SO}_4/\text{KMnO}_4$ -modified CNTs were 20–30 nm (Fig. 2(a–c)).

3.2. pH effects

The adsorption capacity of Cd^{2+} onto the surface of CNTs increased with both the pH of the system from acidic to alkaline and the temperature (Fig. 3(a–c)). pH is one of the most important factors that affect the sites of dissociation of CNTs and the hydrolysis, complexation and precipitation of Cd^{2+} . At acidic pH, the surface is expected to have a net positive charge, and to adsorb few Cd^{2+} ions. Above pH_{iep} , a net

Table 1
Characteristics of as-grown and modified CNTs.

Sample	Purity C (%)	Element O/Ni (%)	pH_{iep}	Surface area (m^2/g)
As-grown	>90	5.4/1.0	4.9	78
MW/ H_2SO_4 process	>90	7.8/0.5	3.8	98
MW/ $\text{H}_2\text{SO}_4/\text{KMnO}_4$ process	>85	12.2/0.5	–	112

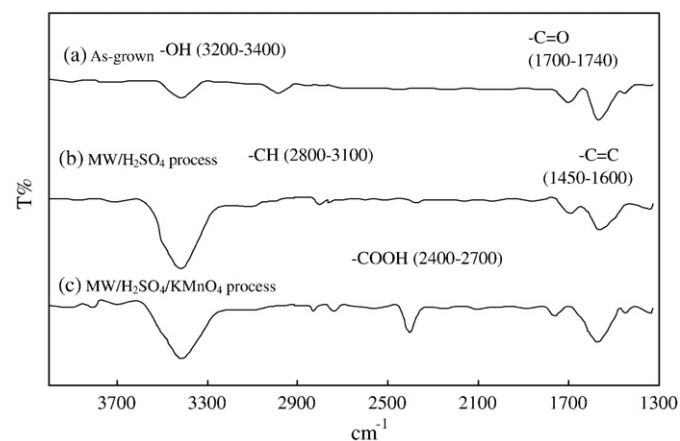


Fig. 1. FTIR spectra of CNTs.

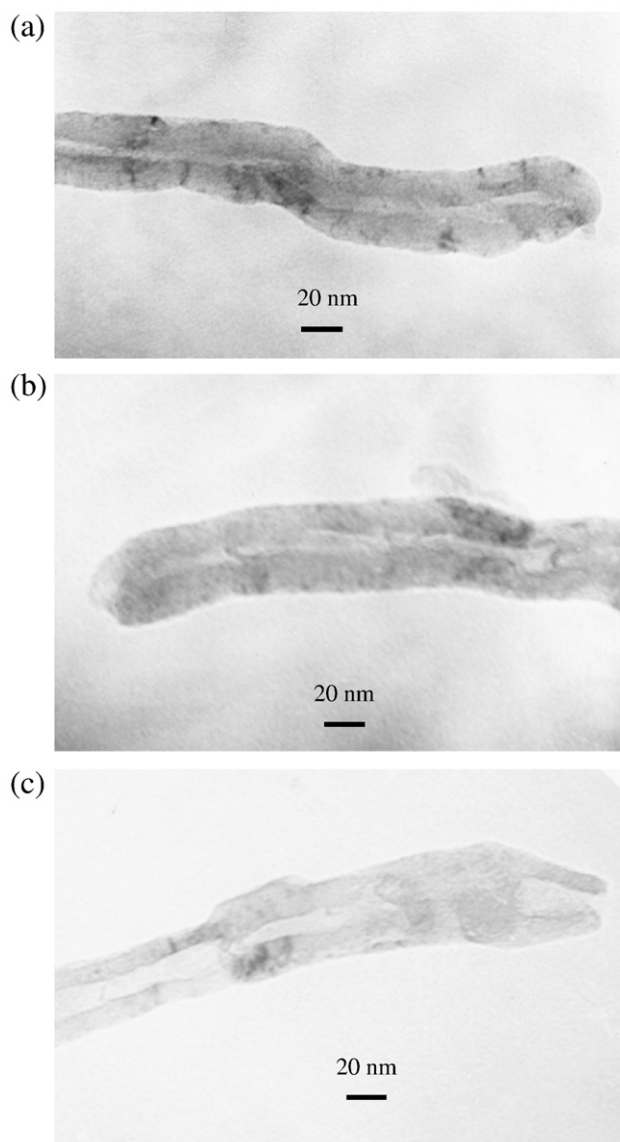


Fig. 2. TEM images of CNTs (a) as-grown CNTs, (b) MW/H₂SO₄ process modified CNTs and (c) MW/H₂SO₄/KMnO₄ process modified CNTs.

negative charge is present on the surface of the CNTs, promoting the adsorption of Cd²⁺, because of the electrostatic force of attraction between Cd²⁺ and the surface of the CNTs. The Cd²⁺ adsorption capacity rapidly increased with pH above 8.5, which in fact can be explained by the precipitation of Cd²⁺ from solution [14,27]. Therefore, the experiments were performed to determine the adsorption isotherms at a fixed pH of 6. At pH values of over pH_{iep}, a net negative charge is present on the surface of the CNTs, promoting the adsorption of Cd²⁺, because of the electrostatic force of attraction between Cd²⁺ and the surface of the CNTs. The MW/H₂SO₄/KMnO₄-modified CNTs had the highest adsorption capacity of the three CNTs of interest. The dependence of adsorption on pH is associated with the dependence of the surface charge on CNTs on pH. For a given pH, the zeta potentials followed the order as-grown CNTs > MW/H₂SO₄-modified CNTs > MW/H₂SO₄/KMnO₄-modified CNTs. Therefore, the adsorption capacity of Cd²⁺ followed the order MW/H₂SO₄/KMnO₄-modified CNTs > MW/H₂SO₄-modified CNTs > as-grown CNTs. This study suggests that modifying the surface of CNTs not only can make it more negatively charged and hydrophilic but can also form various functional groups, substantially promoting the adsorption of Cd²⁺ onto modified CNTs. The previous report [21] also indicated that the functional groups by acid/oxidation improved the ion-exchange

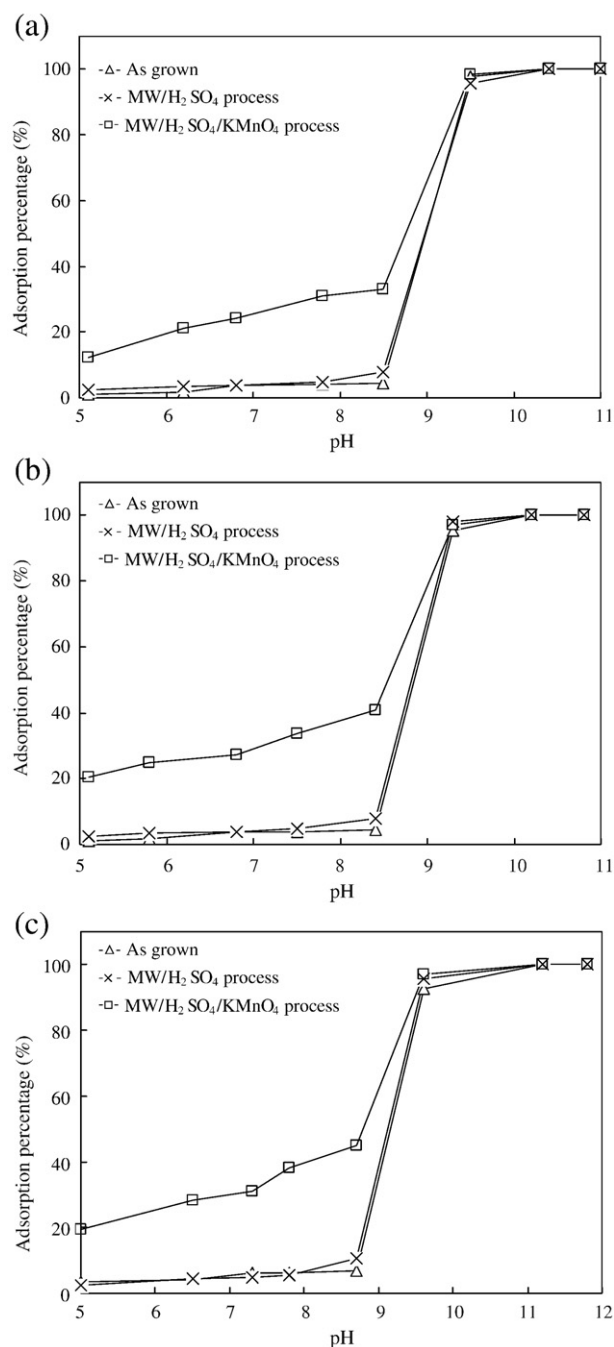


Fig. 3. Effects of pH (a) 290 K, (b) 300 K, and (c) 310 K, (initial Cd²⁺ = 40 mg/l, ionic strength = 0.01 M, CNTs = 0.25 g/l, and contact time = 24 h).

capabilities of the CNTs and increased Cd (II) adsorption capacities correspondingly.

3.3. Kinetic analyses

Fig. 4 presents the kinetic analysis of the adsorption of Cd²⁺ onto as-grown and modified CNTs. Pseudo first- and second-order models and intraparticle diffusion and Bangham's models were tested against the experimental data to explicate the kinetics of the adsorption process. The pseudo first-order and pseudo second-order models are

$$\ln(q_e - q) = \ln(q_e) - k_1 t \quad (1)$$

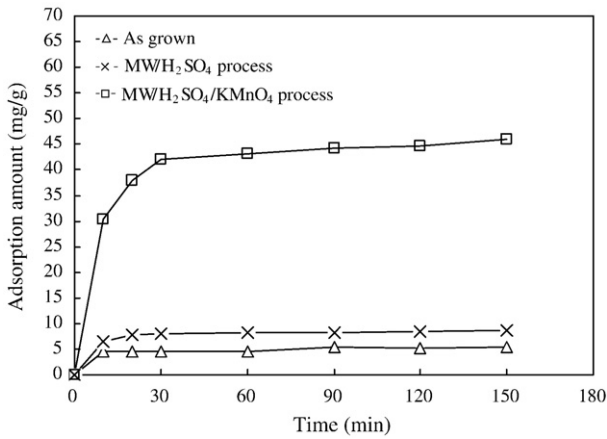


Fig. 4. Effects of adsorption with reaction time (310 K, pH=6, initial Cd²⁺ = 40 mg/l, ionic strength = 0.01 M, and CNTs = 0.25 g/l).

$$\frac{t}{q} = \frac{1}{k_2 q_e^2} + \frac{t}{q_e} \tag{2}$$

where q_e and q are the amounts of Cd²⁺ adsorbed on CNTs at equilibrium and at various times t (mg/g); k_1 is the rate constant of the pseudo first-order model of adsorption (1/h) [28] and k_2 is the rate constant of the pseudo second-order model of adsorption (g/mg h) [29]. The adsorption was rapid during 0.5 h of contact time, and then slowed, because numerous vacant surface sites were available for adsorption during the initial stage, and then, the remaining vacant surface sites could not be easily occupied because of the repulsive forces between the Cd²⁺ molecules on the CNTs and the bulk phase.

The initial adsorption rate h (mg/g h) can be given by $h = k_2 q_e^2$. Since neither the pseudo first-order nor the second-order model yields the diffusion mechanism, the kinetic results were analyzed using the intraparticle diffusion model, which model is given by $q = k_i t^{1/2} + C$, where C is the intercept and k_{BiB} is the intraparticle diffusion rate constant (mg/g h^{0.5}) [30]. Kinetic data were further adopted to determine the slowness of the step in the present adsorption system, using Bangham's model [29,31].

$$\log\left(\frac{C_0}{C_0 - qm}\right) = \log\left(\frac{k_0 m}{2.303V}\right) + \alpha \log t \tag{3}$$

where q and t are defined as in the pseudo first-order model; C_0 represents the initial concentration of Cd²⁺ in solution (mg/l); V is the volume of solution (ml); m is the mass of CNTs per liter of solution (g/l) and k_0 and α are constants.

Table 2 provides the kinetic parameters given which the R^2 value of the pseudo first-order model are 0.54–0.87 and second-order model exceeded 0.989; moreover, the q value ($q_{e, cal}$) calculated from the pseudo second-order model was consistent with the experimental q values ($q_{e, exp}$). Accordingly, this study suggests that the pseudo second-order model best represented the adsorption kinetics (Fig. 5).

Various mechanisms determine the adsorption kinetics; the most limiting mechanisms are the diffusion mechanisms, including external diffusion, boundary layer diffusion and intraparticle diffusion [32]. If the plot of q as a function of $t^{1/2}$ is linear and passes through the origin, then intraparticle diffusion is the sole rate-limiting step [29,33]. Therefore, the intraparticle diffusion model was applied to determine the rate-limiting step of the adsorption process. In Table 2, the R^2 value of regression was 0.54–0.87 and the plot did not pass through the origin, revealing that adsorption involved intraparticle diffusion hardly, and was not the only rate-controlling step. The double logarithmic plot based on Bangham's model was not perfectly linear ($R^2 = 0.522–0.863$)

Table 2 Kinetic parameters for adsorption of aqueous Cd²⁺ by as-grown and modified CNTs.

Pseudo first-order model	$q_{e, exp}$ (mg/g)	k_1 (1/h)	$q_{e, cal}$ (mg/g)	R^2
As-grown	5.5	0.38	1.2	0.542
MW/H ₂ SO ₄ process	8.7	1.02	1.7	0.843
MW/H ₂ SO ₄ /KMnO ₄ process	46.0	1.22	11.7	0.871
Pseudo second-order model	h (mg/g h)	k_2 (g/mg h)	$q_{e, cal}$ (mg/g)	R^2
As-grown	73	2.55	5.4	0.989
MW/H ₂ SO ₄ process	179	2.40	8.6	0.999
MW/H ₂ SO ₄ /KMnO ₄ process	625	0.29	46.3	0.999
Intraparticle diffusion model	k_i (mg/g h ^{0.5})	C (mg/g)	R^2	
As-grown	3.52	0.78	0.623	
MW/H ₂ SO ₄ process	5.95	1.14	0.522	
MW/H ₂ SO ₄ /KMnO ₄ process	34.2	2.57	0.493	
Bangham's model	α	k_0 (l/(mg/l))	R^2	
As-grown	2.1×10^{-3}	1.87	0.522	
MW/H ₂ SO ₄ process	4.5×10^{-3}	1.88	0.826	
MW/H ₂ SO ₄ /KMnO ₄ process	4.4×10^{-2}	2.11	0.863	

so the diffusion of Cd²⁺ into pores of CNTs was not the only rate-controlling step [34].

4. Conclusion

This study examines the equilibrium adsorption of Cd²⁺ onto as-grown and modified CNTs at various pH values and temperatures. The MW/H₂SO₄ and MW/H₂SO₄/KMnO₄ modifications reduced the p*H*_{IEP} by

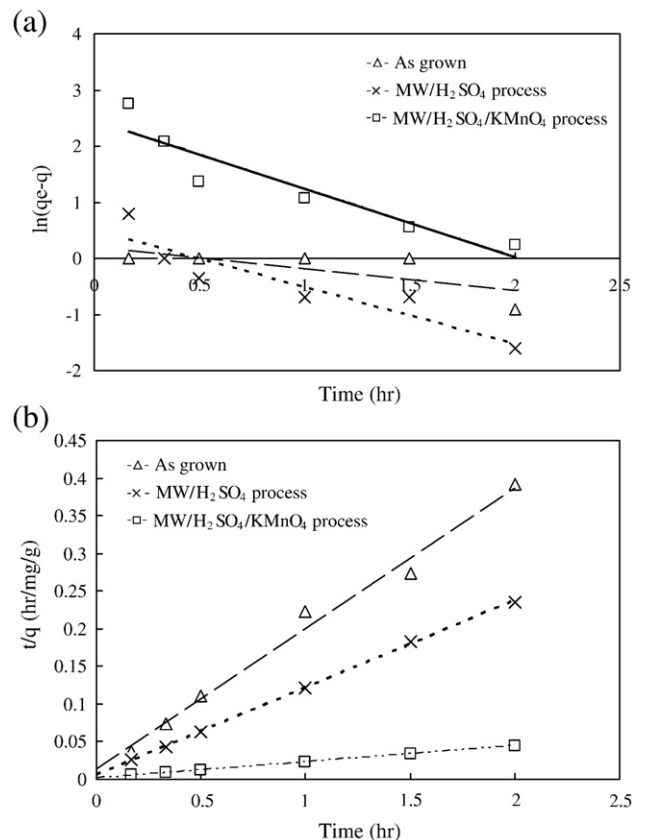


Fig. 5. Regressions of adsorption reaction rate (a) pseudo first-order, and (b) pseudo second-order.

the formation of some functional groups. The adsorption capacity of aqueous cadmium (II) onto as-grown and modified CNTs increased with the pH and temperature. The negatively charged surfaces of modified CNTs electrostatically favored the adsorption of Cd^{2+} in $\text{MW}/\text{H}_2\text{SO}_4/\text{KMnO}_4$ -modified CNTs more than in $\text{MW}/\text{H}_2\text{SO}_4$ -modified CNTs. At a particular pH, the adsorption capacity of Cd^{2+} of the $\text{MW}/\text{H}_2\text{SO}_4/\text{KMnO}_4$ -modified CNTs exceeded that of $\text{MW}/\text{H}_2\text{SO}_4$ -modified CNTs and as-grown CNTs. The kinetic analyses of adsorption were performed using pseudo first- and second-order models and the regression results indicated that a pseudo second-order model more accurately captured the adsorption kinetics.

Acknowledgements

The authors would like to thank the National Science Council of the Republic of China, Taiwan, for financially supporting this research under Contract No. NSC 97-2622-E-224-001-CC3. Additionally, Mr. Tan is appreciated for assistance in conducting some of the experiments.

References

- [1] C.N. Mulligan, R.N. Yong, B.F. Gibbs, *Eng. Geol.* 60 (2001) 193–207.
- [2] A. Corami, S. Mignardi, V. Ferrini, *J. Colloid Interface Sci.* 317 (2008) 402–408.
- [3] S. Mandjiny, K.A. Matis, A.I. Zouboulis, M. Fedoroff, J. Jeanjean, J.C. Rouchaud, N. Toulhoat, V. Potocek, C. Loos-Neskovic, P. Maireles-Torres, D. Jones, *J. Mater. Sci.* 33 (1998) 5433–5439.
- [4] M. Kazemipour, M. Ansari, S. Tajrobehkar, M. Majdzadeh, H.R. Kermani, *J. Hazard. Mater.* 150 (2008) 322–327.
- [5] M. Koby, E. Demirbas, E. Senturk, M. Ince, *Bioresour. Technol.* 96 (2005) 1518–1521.
- [6] D. Marchat, D. Bernache-Assollant, E. Champion, *J. Hazard. Mater.* A139 (2007) 453–460.
- [7] A. Ozer, H.B. Pirincci, *J. Hazard. Mater.* B137 (2006) 849–855.
- [8] J.W. Shim, S.J. Park, S.K. Syr, *Carbon* 39 (2001) 1635–1642.
- [9] N. Zhang, J. Xie, V.K. Varadan, *Smart Mater. Struct.* 11 (2002) 962–965.
- [10] Y.H. Li, J. Ding, Z. Luan, Z. Di, Y. Zhu, C. Xu, D. Wu, B. Wei, *Carbon* 41 (2003) 2787–2792.
- [11] X. Peng, Z. Luan, Z. Di, Z. Zhang, C. Zhu, *Carbon* 43 (2005) 855–894.
- [12] C.S. Lu, H.S. Chiu, *Chem. Eng. Sci.* 61 (2006) 1138–1145.
- [13] J. Liu, M.R. Zubiri, B. Vigolo, M. Dossot, Y. Fort, J.J. Ehrhardt, E. McRae, *Carbon* 45 (2007) 885–891.
- [14] C.H. Wu, *J. Colloid Interface Sci.* 311 (2007) 338–346.
- [15] C.Y. Kuo, *J. Hazard. Mater.* 152 (2008) 949–954.
- [16] F. Liang, A.K. Sadana, A. Peera, J. Chattopadhyay, Z. Gu, R.H. Hauge, W.E. Billups, *Nano Lett.* 4 (2004) 1257–1260.
- [17] C.A. Dyke, J.M. Tour, *J. Am. Chem. Soc.* 125 (2003) 1156–1157.
- [18] M. Holzinger, J. Abraham, P. Whelan, R. Graupner, L. Ley, F. Hennrich, M. Kappes, A. Hirsch, *J. Am. Chem. Soc.* 125 (2003) 8566–8580.
- [19] V. Georgakilas, K. Konstantinos, M. Prato, D.M. Guldi, M. Holzinger, A. Hirsch, *J. Am. Chem. Soc.* 124 (2002) 760–761.
- [20] S. Caddick, *Tetrahedron Asymmetr.* 51 (1995) 10403–10432.
- [21] Y.H. Li, S. Wang, Z. Luan, J. Ding, C. Xu, *Carbon* 41 (2003) 1057–1062.
- [22] Y.H. Li, Y. Zhu, Y. Zhao, D. Wu, Z. Luan, *Diam. Relat. Mater.* 15 (2006) 90–94.
- [23] M. Monthieux, B.W. Smith, B. Burteaux, A. Claye, J.E. Fischer, D.E. Luzzi, *Carbon* 39 (2001) 1251–1272.
- [24] W.M. Davis, C.L. Erickson, C.T. Johnston, J.J. Defino, J.E. Porter, *Chemosphere* 38 (1999) 2913–2928.
- [25] C.S. Lu, Y.L. Chung, K.F. Chang, *Water Res.* 39 (2005) 1183–1189.
- [26] C. Yang, X. Hu, D. Wang, C. Dai, L. Zhang, H. Jin, S. Agathopoulos, *J. Power Sources* 160 (2006) 187–193.
- [27] A.S. Ozcan, B. Erdem, A. Ozcan, *J. Colloid Interface Sci.* 280 (2004) 44–54.
- [28] S. Lagergren, K. Sven, *Vetenskapsakad. Handl. Band* 24 (1898) 1–39.
- [29] G. Blanchard, M. Maunay, G. Martin, *Water Res.* 18 (1984) 1501–1507.
- [30] W.J. Weber Jr., J.C. Morris, *J. Sanit. Eng. Div. ASCE* 89 (1963) 31–59.
- [31] C. Aharoni, S. Sideman, E. Hoffer, *J. Chem. Technol. Biotechnol.* 29 (1979) 404–412.
- [32] E. Guibal, P. McCarrick, J.M. Tobin, *Sep. Sci. Technol.* 38 (2003) 3049–3073.
- [33] A. Ozcan, A.S. Ozcan, *J. Hazard. Mater.* 125 (2005) 252–259.
- [34] E. Tutem, R. Apak, C.F. Unal, *Water Res.* 32 (1998) 2315–2324.